



Comparison between gelatin/carboxymethyl cellulose and gelatin/carboxymethyl nanocellulose in tramadol drug loaded capsule



Ghada Kadry*

Chemical Engineering Department, The Higher Institute of Engineering, Alshrouk Academy, Egypt

ARTICLE INFO

Keywords:

Natural product chemistry
Pharmaceutical chemistry
Drug delivery systems
Interpenetrating networks
Morphology
Nano-particles- carboxymethyl cellulose

ABSTRACT

The comparison between Tramadol drug loaded microspheres prepared from gelatin/sodium carboxymethyl cellulose (NaCMC) and those prepared from gelatin/sodium carboxymethyl nanocellulose (NaCMNC) in presence of glutaraldehyde (GA) as cross linker was carried out. Cellulose isolated from rice straw was hydrolyzed using 65% H₂SO₄ to prepare nanoparticles with average particle size ranging from 44 to 66 nm. Various formulations of gelatin/NaCMC and gelatin/NaCMNC were prepared with different ratios of amounts of gelatin, NaCMC/NaCMNC, and GA. Microspheres were characterized by fourier transform infrared (FTIR) spectroscopy and scanning electron microscopy. The FTIR spectroscopy results confirmed the structure of microsphere and the absence of chemical interactions among Tramadol drug, polymer, and crosslinking agent. The ultraviolet spectroscopy showed 68% efficiency of the drug encapsulation using cellulose, while 55% for nanocellulose. The equilibrium water uptake decreased from 646 to 329% for cellulose microspheres, when the amount of GA increased from 5 to 10 mL. In contrast, the equilibrium water uptake decreased significantly from 501 to 33.7% for nanocellulose microspheres. The yield percentage enhanced from 54.67 to 80% for nanocellulose microspheres. The *in vitro* release rate was also calculated. The percent cumulative release of drug was significantly increased at the first 2 h and then a slow increase was further noticed. In general, the nanocellulose microsphere showed lower release rates than cellulose. None of the prepared microsphere presented 100% drug release until 12 h.

1. Introduction

Drug delivery systems can exactly control the release rates or target drugs to a specific body site, thus having an important impact on the healthcare system. The pharmaceutical industry has viewed advancement in an interaction between the fields of polymer and material science, for the development of the novel drug delivery systems [1, 2, 3, 4]. Carrier technology has proposed an intelligent technique for drug delivery by coupling the drug to a carrier particle such as microspheres, nanoparticles, liposomes, etc. [5, 6, 7], which modulates the release and absorption characteristics of the drug [8]. Microspheres constitute an important part of these particulate drug delivery systems by virtue of their small size and efficient carrier characteristics [9, 10, 11]. The novel drug delivery systems are effective in transport of drug molecules to the target cells or tissues and release them in a controlled manner. Although the drug release system provides extended periods of active drug blood

levels that help in the improvement of patient compliance, it has limitation of short residence time at the site of absorption [12, 13, 14, 15, 16, 17, 18]. This issue can be solved by providing an intimate contact of the drug delivery systems with the absorbing membranes [19]. The modification of releasing drug system has been reported in pharmaceutical literature [19, 20, 21].

Polymers are used as blenders to achieve sustained release [22, 23, 24]. Moreover, in recent years the natural carbohydrate polymers have been used in the applications of biomedical and pharmaceutical science attributed to their biocompatibility and biodegradability. Rice straw is an agricultural byproduct that is burned soon after threshing to get rid of it and to prepare the soil for the next crop. In Egypt the uncontrolled burning of huge amounts of rice straw causes severe air pollution, namely "Black Cloud". Therefore, alternate techniques should be designed to use rice straw as raw material to minimize air pollution. Cellulose is extracted from rice straw by alkaline pulping process or acidic pulping

* Corresponding author.

E-mail address: kadryghada@yahoo.com.

process [25, 26, 27, 28]. Cellulose derivatives are hydrophilic polymers and have the ability to form gels in aqueous medium. It can help in the development of controlled release technology in the formulation of pharmaceutical products [29, 30]. Cellulose is a natural organic polymer. It is a linear chain homopolymer with 1,4-D-glucose molecules linked together. Hydrolysis of cellulose can be carried out chemically by using strong acids or biologically by using enzymes such as cellulase. Native cellulose can be broken into micro- and nanocrystalline structures by the effect of strong acids or mechanical forces. Acid hydrolysis process of cellulose is used to breakdown the amorphous regions of cellulose, which enables the separation of nanocrystalline cellulose (NC) [31, 32, 33, 34, 35, 36]. NC cellulose is considered as a novel cellulosic material due to its excellent characteristics including biodegradability, nontoxicity, and renewability. Cellulose leads to the enhancement of the mechanical properties especially at the nano-level [37, 38, 39, 40, 41].

On the other hand, gelatin, which is derived from collagen, is a fibrous material that occurs in skin, bones, and connective tissues of animals [42]. It is an edible material, soluble at the body temperature, and becomes gelatinous at temperatures just above ambient. It is used for pharmaceutical applications because of its biocompatibility and biodegradability [43].

Tramadol HCl (TmH) is a synthetic, centrally acting analgesic and is currently approved for use in many countries [44]. It is used for treatment of severe and moderate pain, where it acts as opiate agonist, through selective binding to the μ -opioid receptor, and weak inhibition of norepinephrine and serotonin uptake [45]. However, tramadol has many side effects as well such as vomiting, nausea, sweating, itching, and constipation. Drowsiness has also been reported, although it is less of an issue than for non-synthetic opioids. Patients prescribed tramadol for general pain relief with or without other agents have reported withdrawal symptoms including uncontrollable nervous tremors. Tramadol has half-life of approximately 2.5 h. This study tries to solve this problem by loading the tramadol drug on slow release microsphere polymer, which offers control release and also control side effects of that drug. Slow releases depend on the extent of crosslinking and the amount of carboxymethyl cellulose. Two types of microspheres were prepared, one from gelatin/sodium carboxymethyl cellulose (NaCMC) and the other from gelatin/sodium carboxymethyl nanocellulose (NaCMNC) in the presence of glutaraldehyde (GA) as a cross linker. These two types were synthesized with the objective of controlling the release of the tramadol drug. The structure of polymer network was studied and the absence of chemical interactions among drug, polymer, and crosslinking agent was proved through Fourier Transform Infrared (FTIR) spectroscopy. Moreover, the morphology of the surface of microsphere was studied by scanning electron microscopy (SEM), and percent efficiency of the drug encapsulation and the in vitro release rates were calculated.

2. Experimental

2.1. Materials

Rice straw was used as the biomass raw material source for the natural lignocellulosic fibers and was gained from our local Egyptian farms, where it was dried at room temperature to equilibrium moisture content of 5–6 wt.%. Tramadol was kindly received as a gift sample from Abo Alazaum Hospital, Cairo, Egypt. Gelatin, GA solution (25%, v/v), and n-hexane were purchased from Sigma-Aldrich. *N,N*-dimethyl acetamide (DMAc) and monochloroacetic acid were acquired from Aldrich Chemical Company Inc. (Milwaukee WI, USA). All the chemicals were used as received without any further purification.

The chemical composition of the isolated fibers, i.e. holocellulose, alpha cellulose, Klason lignin, and ash content, were determined according to TAPPI T257 om-85, TAPPI T222 om-88, and TAPPI om-85, respectively [46].

2.2. Methods

2.2.1. Isolation of cellulose from rice straw

Cellulose was obtained from rice straw by an alkaline pulping process. The rice straw was cut approximately to the size of 3 cm, and sodium hydroxide solution (1%, w/w) with liquor ratio 1:10 was added. The pulping process was carried in a rotary autoclave for 2 h at 160 °C as mentioned in literature reports [47, 48, 49], and then the pulp reached neutrality through washing with water. Lignin was removed by two stages of bleaching method. The bleaching process was performed using sodium hypochlorite of 60% active chlorine for 2 h at 40 °C. The liquor ratio (fiber to solution) was 10:1 and the pH was 9 during the bleaching process as mentioned in literature reports [50, 51, 52, 53, 54]. At the end of bleaching process, the bleached cellulosic fibers molecules that comprised a number of reactive hydroxyl groups were washed until neutrality and left to dry in air.

2.2.2. Preparation of cellulose nanoparticles

Cellulose nanocrystals were obtained by hydrolyzing cellulose fibers with 65 wt.% sulfuric acid followed by grinding the produced particulates. Then the particles were washed with distilled water until neutrality and left to dry in oven at 40 °C. The process was discussed in detail in our previous literature report [55]. The average size of the obtained nanocellulose crystals varied from 44 to 66 nm according to transition electron microscopy (TEM) (see Fig. 1).

2.2.3. Preparation of sodium carboxymethyl cellulose

In order to prepare NaCMC, cellulose was dried at 80 °C for 8 h and then sieved using a 0.32 mm screen. Cellulose was soaked in 20% sodium hydroxide solution in a 200-mL beaker. The dispersed solution was heated and stirred at 80 °C for 4.5 h, the residue was filtered, and then washed with 95% ethanol. The residue was relocated into a beaker, then 15% NaOH solution in water bath and chloroacetic acid were added. The reaction was performed at 70 °C for 1 h with stirring. The product was filtered and washed with 75% ethanol solution, and then left in air to dry. The above

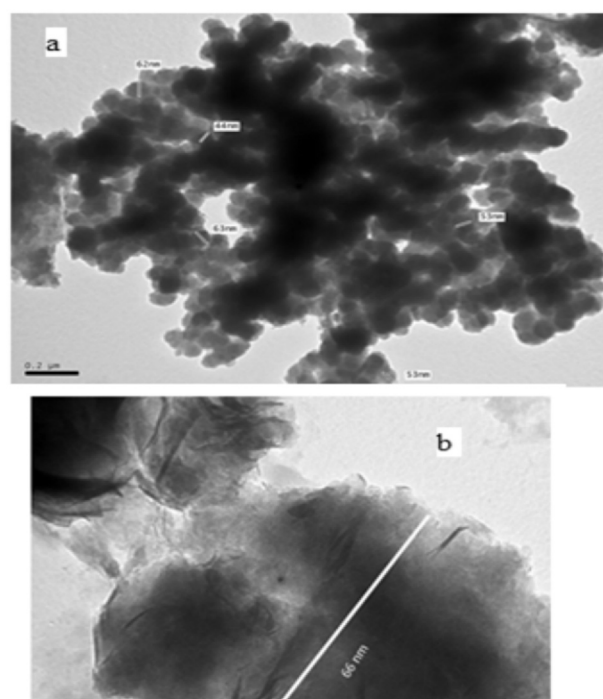


Fig. 1. TEM image of nanocellulose (a) as-formed and (b) single nanoparticle of cellulose.

Table 1
Schematic representation of the synthesis of gelatin/NaCMNC microspheres.

Formation code	NaCMNC % (w/w)	Gelatin % (w/w)	Drug loading %	GA mL
F1	10	90	20	5
F2	10	90	20	10
F3	10	90	40	5
F4	10	90	40	10
F5	20	80	20	5
F6	20	80	20	10
F7	20	80	40	5
F8	20	80	40	10

Table 2
Schematic representation of the synthesis of gelatin/NaCMC microspheres.

Formation code	NaCMC% (w/w)	Gelatin% (w/w)	Drug loading %	GA mL
H1	10	90	20	5
H2	10	90	20	10
H3	10	90	40	5
H4	20	80	40	10
H5	20	80	20	5
H6	20	80	20	10

mentioned procedure was carried on nanocellulose to form NaCMNC.

2.2.4. Synthesis of gelatin/sodium carboxymethyl cellulose microspheres with semi-interpenetrating network

Emulsion-crosslinking method was used to fabricate gelatin/NaCMC microspheres with semi-interpenetrating network (IPN). It was prepared by dissolving gelatin in distilled water at 37 °C with constant stirring to obtain a homogeneous solution. The homogeneous solution was cooled and NaCMC was added. It was stirred overnight; and then Tramadol was added. This was followed by the slow addition of a mixture of petroleum ether and light liquid paraffin (2:3 wt. ratio). The suspended solution was stirred at 400 rpm for 10 min. GA was added slowly with stirring for 2 h. Further, filtration and washing with n-hexane was carried out. The separated microspheres were dried at 40 °C for 24 h under vacuum. The above mentioned procedure was carried out on NC to prepare gelatin/NaCMNC microspheres. The formulations were organized with codes that are represented in Tables 1 and 2.

2.2.5. Evaluation study

2.2.5.1. Product yield. The product yield of the prepared micro-particles was calculated by using Eq. (1) to determine the efficiency of the process:

$$\text{Encapsulation Efficiency} = \frac{\text{Absorbance of microparticles containing 0.05 g Tramadol HCl}}{\text{Absorbance of 0.05 g Tramadol}} \times 100 \quad (2)$$

$$\% \text{ mass loss} = \frac{M_0 - M_1}{M_0} \times 100 \quad (1)$$

where M_0 is the initial weight of drug and polymer and M_1 is the weight of micro-particles.

2.2.5.2. Morphological characteristics of surface of microspheres. SEM (Hitachi, S 3000H, Japan) was used in order to study the morphology of

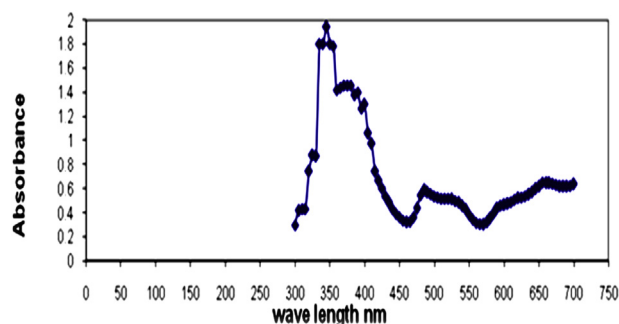


Fig. 2. Determination of λ_{max} of drug at 345 nm.

the micro-particles. The micro-particles were coated with gold using a vacuum evaporator to render them electrically conductive. The coated micro-particles were investigated under a scanning electron microscope at 25 kV to disclose the surface quality.

2.2.5.3. Fourier transform infrared spectral studies. To approve the formation of IPN structure and the chemical stability of the drug in the microspheres, FTIR spectral data were used. The instrument used was a Nicolet spectrometer (Model Impact 410, Milwaukee, WI, USA). The range of scanned spectra was from 4000 to 500 cm^{-1} .

2.2.5.4. Calibration curve of tramadol. A calibration curve is required for the determination of concentration of drug that is released from the microparticles. A known concentration of tramadol in distilled (DI) water was scanned in the range of 200–500 nm using ultraviolet–visible (UV–vis) spectrophotometer. For tramadol having concentration in the range of 0.25–5.5 g L^{-1} , the maximum wavelength, λ_{max} was 345 nm (Fig. 2). The absorbance values at 345 nm obtained with the respective concentrations were recorded and plotted. Fig. 2 shows the calibration curve, indicating that the unknown concentration of tramadol was obtained by knowing the absorbance value.

2.2.5.5. Encapsulation efficiency. Microspheres with specific weight were soaked in water (50 mL) for 30 min, and then stirred for 15 min in order to break the microspheres. Then the solution was centrifuged to remove the polymeric debris. In order to extract all the drug from the sample, the polymeric debris was washed twice with distilled water. The UV spectrophotometer (Secomam, model Anthelie, Paris, France) was used to analyze the clear supernatant solution. The maximum wavelength, λ_{max} was 345 nm (Fig. 2). The encapsulation efficiency was determined by using Eq. (2):

2.2.5.6. Swelling studies. The equilibrium water uptake of IPN microsphere loaded with the drug was calculated. It depended on the swelling water properties of the microsphere. The samples were allowed to swell for 24 h in order to confirm the complete water uptake. The adhered excess surface water was removed by blotting. The electronic microbalance was used to weigh the swollen microspheres to an accuracy of ± 0.01 g. The hydrogel microspheres were then dried in an oven at 60 °C for 5 h until constant weight of dried mass of the samples was obtained. The percent equilibrium water uptake was then calculated by using Eq. (3):

$$\% \text{ Equilibrium water uptake} = \frac{\text{Mass of swollen microsphere} - \text{Mass of dry microsphere}}{\text{Mass of dry microsphere}} \times 100 \quad (3)$$

2.2.5.7. In vitro release studies. Drug release of IPN microspheres was studied in 0.1 N HCl at interval time from 1 to 12 h. *In vitro* release experiments were performed using a magnetic stirrer at Pf 200 rpm. The samples of microsphere loaded with drug were weighed to be around 75.6 mg, and then they were immersed in 100 mL 0.1 N HCl solution at 37 °C. Aliquots of samples were withdrawn at different time intervals and centrifuged. Tramadol concentration was calculated spectrophotometrically at λ_{max} of 345 nm using calibration curve (Fig. 3).

3. Results and discussion

3.1. Isolation of cellulose from rice straw

The result of analysis of rice straw material showed that it contains about 79.33% holocellulose, 13.6% lignin, and 18.4% ash. Thus, the alkaline pulping process was carried out in order to minimize the lignin content to about 5%. Moreover, the holocellulose increased and its content became 81.2%. After pulping, bleaching process was carried out when about 63.4% of pure cellulose with 0.08% of lignin content was obtained.

On the other hand, the reaction for the preparation of NaCMC or NaCMNC proceeded in two steps. In the first step, cellulose or

nanocellulose was suspended in alkali to open the bound cellulose or nanocellulose chains, thus allowing water to enter. Once this happened, cellulose or nanocellulose was then reacted with sodium monochloroacetate to yield sodium carboxymethyl cellulose.

3.2. Fourier transform infrared absorption bands of sodium carboxymethyl cellulose

Fig. 4 shows the FTIR spectra of NaCMC and NaCMNC in the range of 4000–400 cm^{-1} . The spectra of the prepared NaCMC and NaCMNC present a typical characteristic of carboxymethyl cellulose. The band at 3452 cm^{-1} corresponds to O–H stretching vibrations for NaCMNC and at 3520 cm^{-1} corresponds to that in NaCMC. The bands at 2928 and 2935 cm^{-1} represent aliphatic C–H stretching vibrations for NaCMNC and NaCMC, respectively. The asymmetric and symmetric stretching of the carboxylate group bands are shown at 1610 and 1430 cm^{-1} for NaCMNC and 1700 and 1420 cm^{-1} for NaCMC. Finally, peaks at 1074 and 1075 cm^{-1} represent the C–O–C stretching vibration for NaCMNC and NaCMC, respectively. Absorption bands are summarized in Table 3.

Moreover, in order to confirm the drug loading and the crosslinking of gelatin chains by GA, the FTIR spectral data were used. According to literature, FTIR spectrum of gelatin shows peaks at 3413 cm^{-1} for N–H

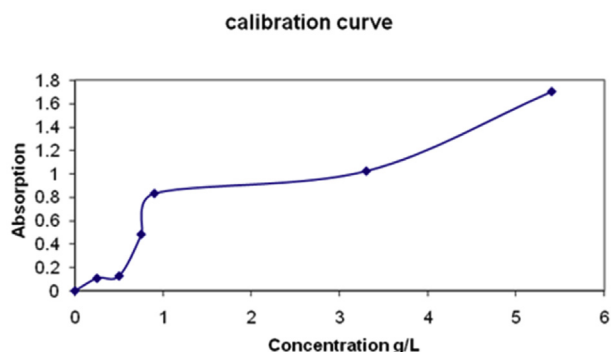


Fig. 3. Calibration curve of different concentrations of pure tramadol drug.

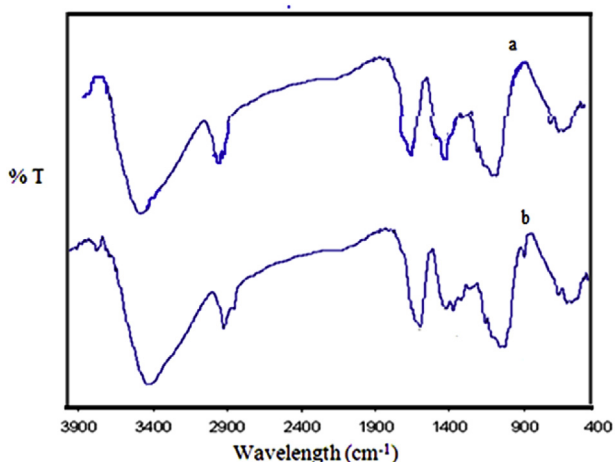


Fig. 4. FTIR spectra of: (a) NaCMC and (b) NaCMNC.

Table 3
FTIR absorption bands of NaCMNC and NaCMC.

Assignment	Peak position, cm^{-1}	
	NaCMNC	NaCMC
O–H stretching	3452	3520
aliphatic C–H stretching	2928	2935
Asymmetric and symmetric stretching of the carboxylate group.	1610 and 1430	1700 and 1420
C–O–C stretching vibration	1074	1075

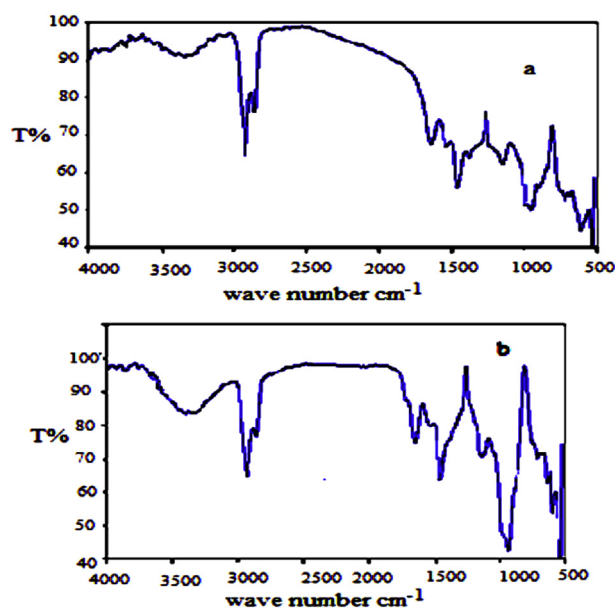


Fig. 5. FTIR spectra of drug loaded microspheres: (a) Gelatin/NaCMC and (b) Gelatin/NaCMNC.

Table 4

FTIR spectral data of tramadol drug loaded microspheres: (a) Gelatin/NaCMC and (b) Gelatin/NaCMNC.

Assignment	Peak position, cm^{-1}	
	Gelatin/NaCMC	Gelatin/NaCMNC
Imine group (C=N) stretching.	1647	1647
O–H stretching.	3431	3431
Aliphatic C–H stretching.	2669	2956
Aliphatic C–H bending.	1440	1450
C–O–C stretching vibration.	1070	1060
Aromatic C–H bending.	726	726
Aromatic C–H stretching.	2956	2919
Monosubstituted phenyl ring.	660	660

stretching, 1535 cm^{-1} for N–H bending, 1646 cm^{-1} for amide, and 1338 and 1239 cm^{-1} corresponding to C–N bond stretching. However, the FTIR peaks for the tramadol drug are present at 3357 cm^{-1} for N–H and O–H stretching; 1610 , 1586 , and 1561 cm^{-1} for aromatic ring stretching, and 896 cm^{-1} indicates the monosubstituted phenyl ring. In the case of tramadol drug-loaded microspheres, all the absorption bands responsible for both gelatin and NaCMC or NaCMNC appear with the addition of new peaks responsible for the loaded drug, as shown in Fig. 5 and Table 4. Absorption band at 1647 cm^{-1} is observed indicating the C=N stretching vibration of the imine group. This band confirms the formation of crosslink between gelatin chains by GA. Band at 1647 cm^{-1} with increased intensity, is observed, which overlaps with that of the amide band of gelatin. The chemical stability of tramadol loaded in microsphere was confirmed by the FTIR spectral data as presented in Fig. 5 and Table 4. The appearance of the bands at 3431 , 2669 , 2956 , 1647 , 1440 , 1450 , 1070 , 1060 , 726 , and 660 cm^{-1} (Table 4) approved the presence of the drug loaded in microspheres and the chemical stability of tramadol even after its encapsulation. The reaction mechanism of the formation of semi-IPN is demonstrated in Fig. 6 that was confirmed by FTIR spectral data.

The SEM images of IPN surface morphology are shown in Fig. 7a, and the entire view depicts a complete microcapsule. Fig. 7b and c demonstrate that when microspheres are placed in drying vacuum, they extrude each other and the shape changes from spherical to polygon [56] due to

the elastic nature of the capsule wall. This results in compact arrangement of the microspheres [57]; however, the as-constructed structure acquires pores and it becomes loose. Moreover, pores are extensively interconnected with increasing porosity. The percentages of gelatin and drug solution play an important role in deciding the porosity of the microspheres [58]. Fig. 7d shows the SEM image, demonstrating the rupture of the microsphere after release of the tramadol drug.

3.3. Encapsulation efficiency

The tramadol loaded semi-IPN gelatin/NaCMNC microspheres with cross linker GA were investigated. The percent yields of the product ranged from 86 to 72.37% and the percent of encapsulation efficiencies was between 8.8 and 55%, as presented in Table 5. However, the product yield of gelatin/NaCMC was in the range from 15.45 to 91.34%, and the percent encapsulation efficiency was between 28.9 and 68% as presented in Table 6. The encapsulation efficiency depends on the leaching out of the drug particle due to the formation of fixed network and the effect of the amount of NaCMC that was observed.

3.4. Swelling studies

Tables 7 and 8 summarize that the percentage of equilibrium water uptake of IPN gelatin/NaCMNC is lower than that of gelatin/NaCMC microspheres. The effect of crosslinking plays an important role in swelling properties of microsphere. With the increase in the quantity of GA from 5 to 10 mL in the gelatin/NaCMNC polymer matrix, the percentage water uptake decreases from 50% for F1 to 45.9% for F2; from 40.7% for F3 to 33.7% for F4; and from 386.97% for F5 to 375.9% for F6, which is related to the rigid network structure formed due to high intensity of crosslinking. The percentage water uptake of F7 decreases significantly from 501.214 to 376.67% compared to F8 with the higher content of cross linker, which indicates higher crosslinking density. It is an evidence of the decrease in the values of the percentage equilibrium water uptake with an increasing amount of GA, and the high content of GA causes the formation of the rigid network structure. The hydrophilic nature of NaCMNC increases with increase in the amount of NaCMNC as presented in Table 7, which improves the water transport rate in addition to the increase of the water uptake capacity of the microspheres. With the

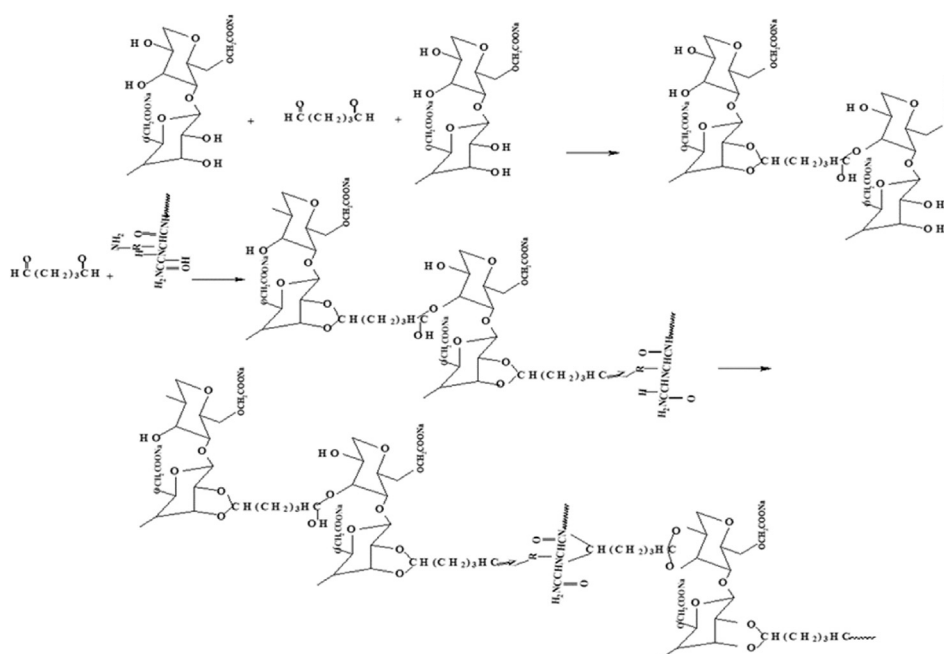


Fig. 6. The reaction mechanism of the formation of semi-IPN.

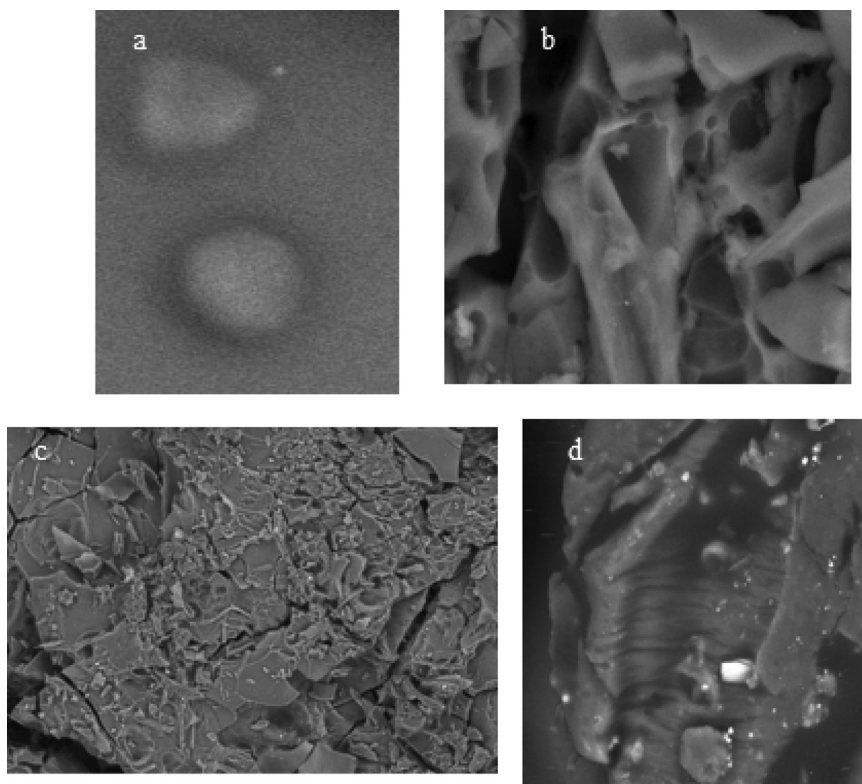


Fig. 7. SEM images of the produced microspheres: (a) Complete microcapsule, (b) The porosity of microsphere, (c) The extrusion of microspheres and the change in shape from spherical into polygon, and (d) The microsphere after releasing the drug.

increase in the percentage water uptake from 50 to 501% for F1 to F7, this result was confirmed for gelatin/NaCMC microspheres equilibrium for which the water uptake decreased from 646% for H1 to 520% for H2; from 520.67% for H3 to 507.9% for H4; and from 385.19% for H5 to 329.23% for H6 as presented in [Table 8](#).

3.5. *In vitro* release studies

[Fig. 8](#) clearly demonstrates that the percentage cumulative release of drug increases significantly for up to 2 h and then increases slowly. However, none of the formulations showed 100% drug release till 8 h for

Table 5
Effect of different formulations on the properties of gelatin/NaCMNC microsphere.

Formulation code	Theoretical yield wt. of drug loaded microsphere (g)	Actual yield wt. of drug loaded microsphere (g)	Mass loss (%)	Product yield (%)	Encapsulation efficiency (%)
F1	5.2	4.19	19.4	80.6	44
F2	8	5.79	27.63	72.37	25.8
F3	5.6	4.31	21.96	78.04	24.4
F4	8.4	6.69	20.36	79.64	25.6
F5	4	3.44	14	86	55
F6	6.8	5.65	16.91	83.1	15.18
F7	4.2	3.47	17.38	82.62	8.8
F8	7	5.45	22.14	77.86	14.08

Table 6
Effect of different formulations on the properties of gelatin/NaCMC microsphere.

Formulation code	Theoretical yield wt. of drug loaded microsphere (g)	Actual yield wt. of drug loaded microsphere (g)	Mass loss (%)	Product yield (%)	Encapsulation efficiency (%)
H1	4.9	2.9	40.81	60	66.39
H2	7.7	1.19	84.54	15.45	61.35
H3	5.6	3.62	35.35	64.6	68
H4	8.4	4.82	42.61	57.38	25
H5	5.2	4.75	8.65	91.34	55
H6	8	3.15	60.6	39.3	28.9

Table 7

The percentage equilibrium water uptake data of the cross linked gelatin/NaCMNC microspheres.

Formulation code	Mass of dry microspheres (g)	Mass of swollen microspheres (g)	Water up taken (w/w%)
F1	0.082	0.123	50
F2	0.0699	0.102	45.92
F3	0.086	0.115	40.7
F4	0.045	0.066	33.7
F5	0.05	0.2532	386.97
F6	0.0614	0.299	375.9
F7	0.0494	0.297	501.214
F8	0.00535	0.255	376.635

Table 8

The percentage equilibrium water uptake data of the cross linked gelatin/NaCMC microspheres.

Formulation code	Mass of dry microspheres (g)	Mass of swollen microspheres (g)	Water up take (w/w %)
H1	0.0353	0.2636	646.74
H2	0.0179	0.111	520.67
H3	0.0329	0.2	507.9
H4	0.172	0.103	495.37
H5	0.0412	0.1999	385.194
H6	0.0260	0.1116	329.23

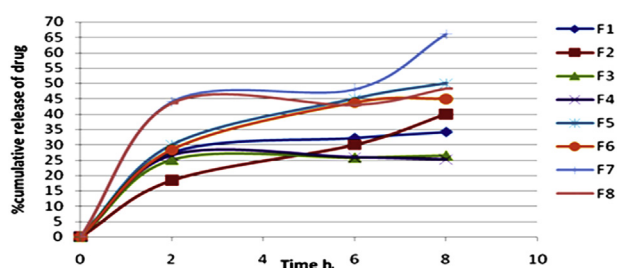


Fig. 8. The percentage cumulative drug release of gelatin/NaCMNC microspheres.

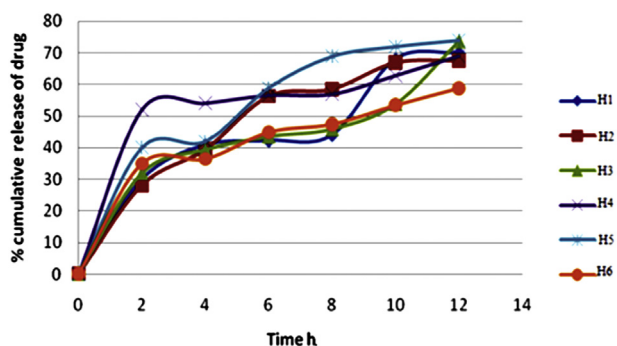


Fig. 9. The percentage cumulative drug release of gelatin/NaCMC microspheres.

gelatin/NaCMNC, and 12 h for gelatin/NaCMC as shown in Fig. 9. In case of gelatin/NaCMNC, nanocellulose microspheres show lower release rates due to the reduction of the penetration of water molecules into the polymer, thus leading to the reduction of swelling of microspheres and slower release of tramadol. Comparative analysis indicates that the cumulative release of drug for gelatin/NaCMNC reaches 66% (Fig. 8), while it reaches 76% for gelatin/NaCMC under the same conditions as presented in Fig. 9. Fig. 8 demonstrates the effect of crosslinking on gelatin/NaCMNC, where F5 shows higher release rate than F6. As a result of the formation of a rigid network structure with higher degree of crosslinking that controls the release rate, this result was confirmed for F7 that showed higher release rate compared to F8. Moreover, F3 showed higher percentage cumulative release than F4.

Effects of NaCMNC are clear in the formulations F1, F5, F3, and F7. The release rate increased with the increase of the NaCMNC content in the IPN microsphere that depended on the hydrophilic nature of NaCMNC and responsible for increasing the swelling properties of microspheres. This result was confirmed by comparing F5 with F1 and F7 with F3.

The drug loading effect on *in vitro* release rates was investigated with respect to formulations F1, F3, F5, and F7. The F7 shows higher rates than F6. This indicates that release rates depend upon the quantity of drug loaded in the polymer matrix. Similarity, F3 exhibits higher release rate than F1, although the release rate increases slightly in F3.

For gelatin/NaCMC, percentage cumulative release is shown in Fig. 9. By increasing the time up to 12 h, the percentage cumulative release increases in all the formulations up to 75%. For H1 the cumulative release increases from 33 to 70% for first 2 h, for H2 it increases from 29 to 68%, for H3 from 32 to 73%, for H4 from 52 to 70%, for H5 from 52 to 70%, and for H6 from 35 to 60%.

Comparative analysis of H1, H3, H4, and H6 reveals the effect of crosslinking. The H6 microsphere shows lower percentage cumulative release than F4, owing to the formation of a rigid network structure with high density of crosslinking. However, the H1 and H3 microspheres exhibited the similarity in drug release rate.

Effects of NaCMC content in formulations H1, H5, H2, and H6 were investigated. The results indicated that the releasing rate was higher in case of H5 than in H1. This is attributed to the increase in the NaCMC content in the polymer matrix, and also the increase in the swelling of the matrix due to the extremely hydrophilic nature of NaCMC. Similarly, H6 shows higher release rates than H2.

The *in vitro* release rates are affected by the amount of drug loading as presented for formulations H1, H3, H2, and H4. The H4 has higher release rates than H2. Moreover, the content of drug in the microsphere also affects the releasing rates. Thus, H3 has higher releasing rate than H1.

Herein, comparison was carried out between this study and other literature studies as shown in Table 9.

4. Conclusions

Cellulose was extracted from rice straw by hydrolysis process. Transition electron microscopy (TEM) was used to investigate the nanostructure of nanocellulose. Two forms of semi-interpenetrating polymer network (IPN) microspheres were synthesized, namely gelatin/NaCMC and gelatin/NaCMNC. Glutaraldehyde (GA) was used as a crosslinker. Tramadol was successfully encapsulated into the synthesized IPN microspheres. The reaction mechanism was proposed and confirmed by FTIR spectroscopy. Microspheres were characterized by FTIR spectroscopy and scanning electron microscopy (SEM). The UV spectroscopic analysis showed 55% encapsulation efficiency for gelatin/NaCMNC and 68% for gelatin/NaCMC microparticles. The *in vitro* release of microspheres was studied depending on the releasing rate. The results

Table 9
Comparison between this study and the other related studies.

Comparison	This study	Study 1	Study 2	Study3
Title	Comparison between gelatin/ carboxymethyl cellulose and gelatin/ carboxymethyl nanocellulose with respect to tramadol drug loaded capsule	CMC/gelatin Blends loaded with Piroxicam: Preparation, characterization, and evaluation of <i>in Vitro</i> release Profile [59]	Iron cross-linked carboxymethyl cellulose-gelatin complex coacervate beads for sustained drug delivery [60]	Preparation and evaluation of gelatin/ sodium carboxymethyl cellulose polyelectrolyte complex micro particles for controlled delivery of isoniazid [61]
Aim	To compare two types of microspheres gelatin/carboxymethyl cellulose and gelatin/carboxymethyl nanocellulose, in controlling the release of the tramadol drug.	To study the effect of the semi-IPN matrix of CMC/gelatin Blends composition on encapsulation and study the kinetic behavior of the release of the piroxicam drug.	To study the <i>vitro</i> release of ibuprofen from Iron cross-linked carboxymethyl cellulose-gelatin complex coacervate	To investigate the optimal conditions for the formation of microparticles of gelatin/ sodium carboxymethyl cellulose thus the dependence of drug encapsulation efficiency and release on the reaction conditions.
Material	all the chemicals were prepared in our lab NaCMC- NaCMNC- and analyzed by FTIR	The author in (1) has purchased the chemicals used of CMC and cellulose and didn't mention the physical and chemical analysis	The author (2) has purchased the chemicals used of CMC and cellulose and didn't mention the physical and chemical analysis -GA not used as a cross linker but ferric chloride	The author in (3) has purchased the chemical used of CMC and cellulose, and didn't mention the physical and chemical analysis
Preparation	Emulsion-crosslinking method using distilled water as dispersing phase	Emulsion-crosslinking method using distilled water as dispersing phase	Emulsion-crosslinking method without GA but ferric chloride in 2-propanol method using distilled water as dispersing phase	Emulsion-crosslinking method using sunflower oil as dispersing phase
Formulation	Different formulations were obtained depending on wt.% of gelatin and NaCMC or NaCMNC, and cross linker and drug	Different formulations were obtained based on wt.% of CMC, cross linker, and drug	Different formulations were obtained depending on wt.% of CMC, cross linker, and drug	Different formulations were acquired depending on mmol g ⁻¹ cross linker
Product yield	Maximum yield of gelatin/NaCMC reached 86%	None	None	none
Study of the surface morphology of microsphere	Thoroughly and systematically carried out.	Carried out	Carried out	Carried out
Confirmation of the absence of interaction between drug and microsphere	through chemical equation and by FTIR spectroscopy	No chemical equation was used. Matrix-Drug interaction and physical State of active agent (through DSC/XRD)	No chemical equation was used. The stable and crystalline nature of ibuprofen in the beads was confirmed by FTIR spectroscopy and DSC	Chemical equation + FTIR spectroscopy
Encapsulation Efficiency%	68% for gelatin/NaCMC, and 55% for gelatin/NaCMNC microspheres%	Maximum encapsulation efficiency 10.64%	entrapment efficiency reached 98. 5%	Loading efficiency around 60 %
Swelling studies:	Swelling reached 501% for gelatin/ NaCMNC microspheres and 646.74% for gelatin/NaCMNC microspheres	None	None	Water Uptake % reached 700 %
<i>In vitro</i> release studies:	Comparison between percentage cumulative drug release of gelatin/NaCMC microsphere that reached 74% for 12 h and percentage cumulative drug release of gelatin/NaCMNC microsphere reached 66% for 8 h	release kinetics analyses demonstrated that the release process seems to be governed by distinctly kinetic models, considering the composition of the sample. the release can be driven by Fickinianan diffusion	Drug release reached 70% for 48 h	Drug release reached 90% for 48 h

indicated that the percent cumulative release of drug was significantly increased at the first 2 h, and then a slow increase was further observed for each type of microsphere.

Declarations

Author contribution statement

Ghada Kadry: Conceived and designed the experiments; Performed the experiments; Analyzed and interpreted the data; Contributed reagents, materials, analysis tools or data; Wrote the paper.

Funding statement

This research did not receive any specific grant from funding agencies in the public, commercial, or not-for-profit sectors.

Competing interest statement

The authors declare no conflict of interest.

Additional information

No additional information is available for this paper.

Acknowledgements

The authors greatly acknowledge the scientific support from Professor Dr. Waleed Al-Zawawi and Professor Dr. Maha Ibrahim, Cellulose and Paper Department, National Research Center, Dokki, Giza, Egypt.

References

- [1] A. Vohra, C. Patel, P. Kumar, H. Thakkar, Development of dual drug loaded solid self-micro emulsifying drug delivery system: exploring interfacial interactions using QbD coupled risk based approach, *J. Mol. Liq.* 242 (2017) 1156–1168.
- [2] Z. Shariatnia, A. Jalali, Chitosan nanocomposite drug delivery systems designed for the ifosfamide anticancer drug using molecular dynamics simulations, *J. Mol. Liq.* 273 (2019) 346–367.
- [3] A. Laha, C. Sharma, S. Majumdar, Sustained drug release from multi-layered sequentially cross linked electrospun gelatin nanofiber mesh, *Mater. Sci. Eng. C* 76 (2017) 782–786.
- [4] T. Castro, M. Alonso, J. Oliva, A. Luévanos, Porous aerogel and core/shell nanoparticles for controlled drug, *Mater. Sci. Eng. C* 96 (2019) 915–940.
- [5] P. Chanphai, V. Konka, H.A. Tajmir-Riahi, Folic acid–chitosan conjugation: A new drug delivery tool 238 (2017) 155–159.
- [6] H. Kim, J. Yang, K. Kim, U. Shin, Biodegradable and injectable hydrogels as an immunosuppressive drug delivery system, *Mater. Sci. Eng. C* 98 (2019) 472–481.
- [7] Y. Manea, A. Khan, M. Qashqoosh, A. Wani, M. Shahadat, Ciprofloxacin-supported chitosan/polyphosphate nanocomposite to bind bovine serum albumin: its application in drug delivery, *J. Mol. Liq.* 9 (2019) 111337.
- [8] F. Shakeel, N. Haqa, A. Al-Dhfyhan, F. Alanazi, I. Alsarra, Double w/o/w nanoemulsion of 5-fluorouracil for self-nanoemulsifying drug delivery system, *J. Mol. Liq.* 200 (2014) 183–190.
- [9] S. Derazkola, M. Niasari, H. Khojasteh, O. Amiri, S. Ghoreishi, Green synthesis of magnetic Fe₃O₄/SiO₂/HAp nanocomposite for atenolol delivery and in vivo toxicity study, *J. Clean. Prod.* 168 (2017) 39–50.
- [10] M. Shahabi, H. Raissi, Assessment of solvent effects on the inclusion behavior of pyrazinamide drug into cyclic peptide based nanotubes as novel drug delivery vehicles, *J. Mol. Liq.* 268 (2018) 326–334.
- [11] M. Kumari, S. Mondal, P. Sharma, Synthesis, characterization and electrochemical monitoring of drug release properties of dual stimuli responsive mesoporous GdPO₄:Eu³⁺ nanoparticles, *J. Alloy. Comp.* 776 (2019) 654–665.
- [12] G. Craig, S. Brown, D. Lamprou, D. Graham, N. Wheate, Cisplatin-tethered gold nanoparticles that exhibit enhanced reproducibility, drug loading, and stability: a step closer to pharmaceutical approval? *Inorg. Chem.* 51 (2012) 3490–3497.
- [13] P. Chen, B. Cui, X. Cui, W. Zhao, Y. Bu, Y. Wang, A microwave-triggered controllable drug delivery system based on hollow mesoporous cobalt ferrite magnetic nanoparticles, *J. Alloy. Comp.* 699 (2017) 526–533.
- [14] S. Hashemipour, H. Panahi, Fabrication of magnetite nanoparticles modified with copper based metal organic framework for drug delivery system of letrozole, *J. Mol. Liq.* 243 (2017) 102–107.
- [15] D. Yansong, L. Bin, Y. Youyong, AI Egen based drug delivery systems for cancer therapy, *J. Control. Release* 290 (2018) 129–137.
- [16] R. Ziqie, G. Hongyu, I. Liang, Z. Chen, M. Lian, L. Meng, F. Lihong, L.I. Dan, “Carboxymethyl cellulose modified graphene oxide as pH-sensitive drug delivery system”, *Int. J. Biol. Macromol.* (2018) 1184–1192.
- [17] W. Treessuppharat, P. Rojanapanthu, C. Siangsano, H. Manuspiya, S. Ummartyotin, Synthesis and characterization of bacterial cellulose and gelatin-based hydrogel composites for drug-delivery systems, *Biotechnol. Rep. (Amst.)* 15 (2017) 84–91.
- [18] I. Arash, Sh. Hamidreza, Gh. Mohsen, N. Ali, I. Mohammad, S. Maryam, Chitosan nanocapsule mounted cellulose nanofibrils as nanoships for smart drug delivery systems and treatment of avian trichomoniasis, *J. Taiwan Inst. Chem. Eng.* (2018) 1–10.
- [19] S. Constain, Y. Cristhian, M. Roger, P. Vanessa, R. Juanita, Natural gum-type biopolymers as potential modified nonpolar drug release systems, *Carbohydr. Polym.* 189 (2018) 31–38.
- [20] Z. Chen, S. Chengmei, T. Furong, C. Yuezhi, Honeycomb structural composite polymer network of gelatin and functional cellulose ester for controlled release of omeprazole”, *Int. J. Boil Macromol* 105 (Part 3) (2017) 1644–1653.
- [21] V. Gopinath, S. Saravanan, A.R. Al-Maleki, M. Ramesh, V. Jamuna, A review of natural polysaccharides for drug delivery .applications: special focus on cellulose, starch and glycogen, *Biomed. Pharmacother.* 107 (2018) 96–108.
- [22] F.M. Mark (Ed.), *Encyclopedia of Polymer Science and Technology*, 3th ed, John Wiley & Sons, New York, 2003.
- [23] P. Sinko, *Martin’s Physical Pharmacy and Pharmaceutical Sciences*, fifth ed., Lippincott Williams & Wilkins, Baltimore, 2006.
- [24] I. Uchegbu, A. Schatzlein, *Polymers in Drug Delivery*, CRCPress, Boca Raton, 2006.
- [25] R. Sun, J. Tomkinson, Fractional separation and physico-chemical analysis of lignin’s from the black liquor of oil palm trunk fiber pulping, *Separ. Purif. Technol.* 24 (2001) 529–539.
- [26] D. Kaur, N. Bhardwaj, R. Lohchab, A study on pulping of rice straw and impact of incorporation of chlorine dioxideduring bleaching on pulp properties and effluents characteristics, *J. Clean. Prod.* (2018).
- [27] A. Sharma, K. Anupam, V. Swaroop, P. Lal, V. Bist, Pilot scale soda-anthraquinone pulping of palm oil empty fruit bunches and elemental chlorine free bleaching of resulting pulp, *J. Clean. Prod.* 106 (2015) 422–429.
- [28] N. Cordeiro, A. Ashori, Y. Hamzeh, M. Faria, Effects of hot water pre-extraction on surface properties of bagasse soda pulp, *Mater. Sci. Eng. C* 33 (2013) 613–617.
- [29] M. Monier, D. Abdel-Latif, H. Ji, Synthesis and application of photo-active carboxymethyl cellulose derivatives, *J. React. Funct. Polym.* 102 (2016) 137–146.
- [30] R. Williams, T. Reynolds, T. Cabelka, M. Sykora, V. Mahaguna, Investigation of excipient type and level on drug release from controlled release tablets containing HPMC, *Pharm. Dev. Technol.* 7 (2) (2002) 181–193.
- [31] K. Prado, M. S pinacé, Isolation and characterization of cellulose nanocrystals from pineapple crown waste and their potential uses, *Int. J. Biol. Macromol.* 22 (2019) 410–416.
- [32] Z. Wang, Z. Yao, J. Zhou, Y. Zhang, Reuse of waste cotton cloth for the extraction of cellulose nanocrystals, *Carbohydr. Polym.* 157 (2017) 945–952.
- [33] F. Kallel, F. Bettaie, R. Khiari, A. García, J. Bras, C. Semia, Isolation and structural characterization of cellulose nanocrystals extracted from garlic straw residues, *Ind. Crops Prod.* 87 (2016) 287–296.
- [34] W. Chen, H. Yu, Y. Liu, Y. Hai, M. Zhang, P. Chen, Isolation and characterization of cellulose nanofibers from four plant cellulose fibers using a chemical-ultrasonic process, *Cellulose* 18 (2) (2011) 433–442.
- [35] Sh. Rezaezhad, N. Nazanezhad, Gh. Asadpur, Isolation of nanocellulose from rice waste via ultrasonication, *Lignocellulose* 2 (1) (2013) 282–291.
- [36] L. Luduena, F.D. asce, A. Alvarez, I. Stefani, Nanocellulose from rice husk following alkaline treatment to remove silica, *BioResources* 6 (2) (2011) 1440–1453.
- [37] M. Babae, M. Jonoobi, Y. Hamzeh, A. Ashori, Biodegradability and mechanical properties of reinforced starch nanocomposites using cellulose nanofibers”, *Carbohydr. Polym.* 132 (2015) 1–8.
- [38] Y. Tanaka, J.P. Gong, Y. Osada, Novel hydrogels with excellent mechanical Performance”, *Prog. Polym. Sci.* 30 (2005) 1–9.
- [39] P. Builders, A. Bonaventure, A. Tiwalade, L. Okpako, A. Attama, Novel multi-functional pharmaceutical excipients derived from microcrystalline cellulose–starch microparticulate composites prepared by compatibilized reactive polymer blending”, *Int. J. Pharm.* 388 (2010) 159–167.
- [40] S. Wafaa, M. Hassan, M. Sabaa, M. Basha, E. Hassan, S. Fadel, ChitosanNanoparticles/cellulose nanocrystals nanocomposites as a carrier system for the controlled release of repaglinide’, *Int. J. Biol. Macromol.* 111 (2018) 604–613.
- [41] W. Qing, Y. Wang, Y. Wang, D. Zhao, X. Liu, J. Zhu, The modified nanocrystalline cellulose for hydrophobic drug delivery, *Appl. Surf. Sci.* 366 (2016) 404–409.
- [42] Y. Tabata, Y. Ikada, Protein release from gelatin matrices, *Adv. Drug Deliv. Rev.* 31 (1998) 287–301. PMID: 10837630.
- [43] C. Ferdinando, Formulation solutions soft gels, *Pharm. Manufac. Pack.* (2000) 69–73.
- [44] J. Varshosaz, N. Tavakoli, F. Kheirolah, Use of hydrophilic natural gums in formulation of sustained-release matrix tablets of tramadol hydrochloride AAPS, *Pharm. Sci. Tech.* 7 (2006) E168–E174.
- [45] N. Muhammad, A. Ahmad, Development of tramadol microparticles by non-solvent addition method and their in vitro characterization, *Iran. Polym. J. (Engl. Ed.)* 18 (12) (2009) 937–946.
- [46] J. Sun, X. Sun, H. Zhao, R.C. Sun, Isolation and characterization of cellulose from sugarcane bagasse”, *Polym. Degrad. Stab.* 84 (2004) 331–339. Error! Hyperlink reference not valid.

- [47] W. El-Zawawy, M. Ibrahim, Synthesis and characterization of cellulose resins, *Polym. Adv. Technol.* 14 (2003) 623–631.
- [48] M. Ibrahim, W. El-Zawawy, Y. Abdel-Fattah, N. Soliman, F. Agblevor, Comparison of alkaline pulping with steam explosion for glucose production from rice straw, *Carbohydr. Polym.* 83 (2011) 720–726.
- [49] A. Rodríguez, A. Moral, L. Serrano, J. Labidi, L. Jiménez, Rice straw pulp obtained by using various methods, *Bioresour. Technol.* 99 (2008) 2881–2886.
- [50] M. Ibrahim, W. El-Zawawy, Y. tkke, A. Koschella, T. Heinze, Cellulose and microcrystalline cellulose from rice straw and banana plant waste: preparation and characterization, *Cellulose* 20 (2013) 2403–2416.
- [51] M. Ibrahim, W. El-Zawawy, Preparation, characterization, and properties of fast-responding bulk hydrogel and treated bleached banana pulp, *Polym. Adv. Technol.* 15 (2004) 275–283.
- [52] M. Ibrahim, A. Koschellab, G. Kadry, T. Heinze, Evaluation of cellulose and carboxymethyl cellulose/poly(vinylalcohol) membranes, *Carbohydr. Polym.* 95 (2013) 414–420.
- [53] S. Heikal, A. Ibrahim, Bleaching of rice straw paper pulp and possibilities for replacement of sodium hydroxide by ammonium hydroxide during the extraction stage, *J. Appl. Chem. Biotechnol.* 28 (1978) 671–676.
- [54] A. Hamed, M. Ibrahim, A. Abdel-Razek, H. El, Germ, preparation of environment friendly cellulose derivatives and paper from rice straw, *J. Environ. Sci.* 40 (2017).
- [55] G. Kadry, AEF. Abd El-Hakim “Effect of nanocellulose on the biodegradation, morphology and mechanical properties of polyvinylchloride/nanocellulose nanocomposites, *RJPCS* 6 (2015) 659–666. [https://www.rjpbcs.com/pdf/2015_6\(6\)/\[113\]](https://www.rjpbcs.com/pdf/2015_6(6)/[113]).
- [56] Weigang Li, W. Gang, C. Hongzheng, W. Mang, Preparation and characterization of gelatin/SDS/NaCMC microcapsules with compact wall structure by complex coacervation”, *Colloid. Surf. Physicochem. Eng. Asp.* 333 (2009) 133–137.
- [57] D. Runying, W. Gang, L. Weigang, Z. Qiang, L. Xihua, C. Hongzheng, Gelatin/carboxymethylcellulose/dioctyl sulfosuccinate sodium microcapsule by complex coacervation and its application for electrophoretic display”, *Colloid. Surf. Physicochem. Eng. Asp.* 362 (2010) 84–89.
- [58] S. Meng, K. James, S. Patrick, T. Yasuhiko, D. Nagi, E. Mark, F. Wong, K. Kurtis, M. Antonios, Antibiotic-releasing porous polymethacrylate/gelatin/antibiotic constructs for craniofacial tissue engineering, *J. Control. Release* 152 (2011) 196–205.
- [59] V. Buzzi, M. Brudner, T. Wagner, G. Bazzo, A. Pezzin, D. Silva, Carboxymethyl cellulose/gelatin blends loaded with piroxicam: preparation, characterization and evaluation of in vitro release profile, *J. Encapsulation Adsorpt. Sci.* 3 (2013) 99–107.
- [60] G. Huei, S. Muniyandy, T. Sathasivam, A. Veeramachineni, P. Janarthanan, Iron cross-linked carboxymethyl cellulose–gelatin complex coacervate beads for sustained drug delivery *Chemical, Papers* 70 (2016) 243–252.
- [61] N. Devi, T. Maji, Preparation and evaluation of gelatin/sodium carboxymethyl cellulose polyelectrolyte complex microparticles for controlled delivery of isoniazid, *AAPS Pharm SciTech* 10 (2009) 1412–1419.